Supplemental Material

Supplemental Figures

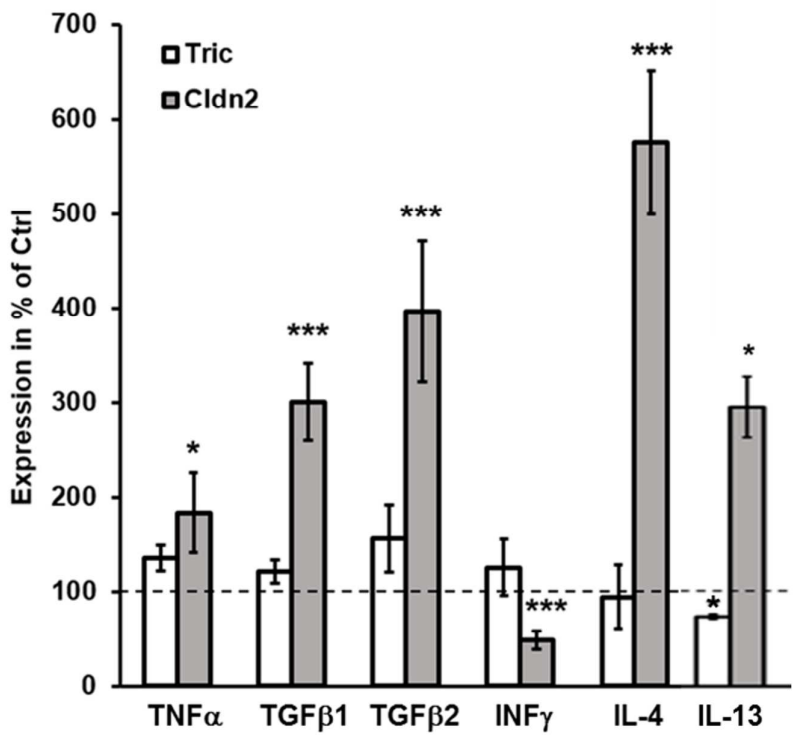

Fig. S1

Effect of other cytokines on tricellulin and claudin-2 expression in HT-29/B6. Densitometric analysis reveals that all other cytokines tested do not influence expression of tricellulin, and that INFγ decreases claudin-2 expression, while all others increase claudin-2 (n=3-12).

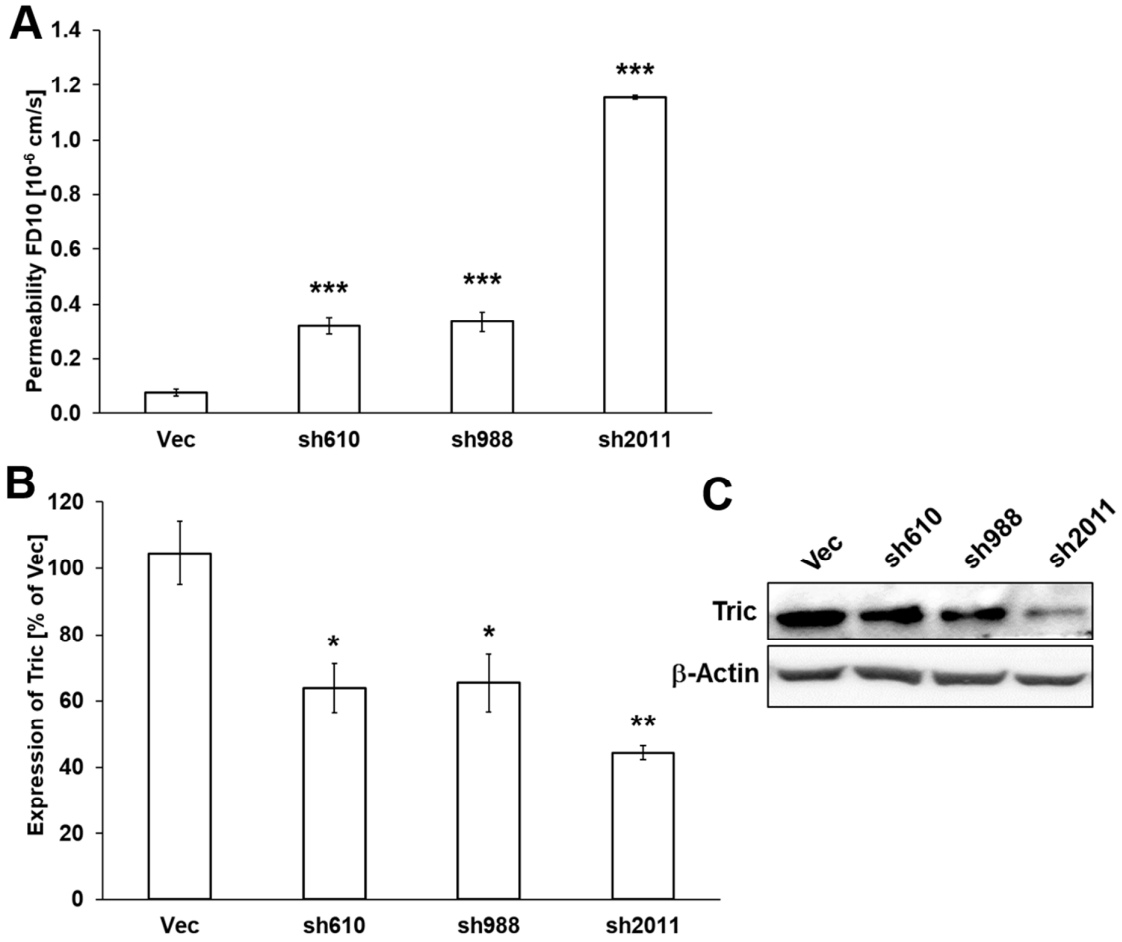

Fig. S2

A. Permeability for the macromolecular paracellular fluxmarker 10 kDa-FITC dextran in shTRIC clones generated using different shRNA constructs (sh610 = TRCN0000072637NM_144724.1-610s1c1TRC 1: sequence 5'- CCG GCC TGA GAT ACT CCT ACA TGA ACT CGA GTT CAT GTA GGA GTA TCT CAG GTT TTT G -3'; sh988 = see main manuscript; sh2011 = TRCN0000072633NM_144724.1-2011s1c1TRC 1; sequence 5'- CCG GGC AGC ATC TAT CAT GTA GAT ACT CGA GTA TCT ACA TGA TAG ATG CTG CTT TTT G -3', Sigma-Aldrich). All three constructs resulted in increased permeability for FD-10 (Vec: 0.08±0.02 · 10^{-6} cm/s, n=6; sh610: 0.32±0.03 · 10^{-6} cm/s, n=6; sh988: 0.34±0.04 · 10^{-6} cm/s, n=4; sh2011: 1.15±0.01 · 10^{-6} cm/s, n=3; ***p<0.001). **B.** Densitometric analysis of protein expression levels in stable shTRIC transfectants in comparison to vector-transfected controls. All shRNA constructs lead to decreased tricellulin expression (Vec: 105±10%, n=10; sh610: 64±8%, n=4; sh988: 65±9%, n=10; sh2011: 44±3%, n=4;**p<0.01,*p<0.05). **C.** Representative western blots showing Tric expression in the different shRNA transfectants.

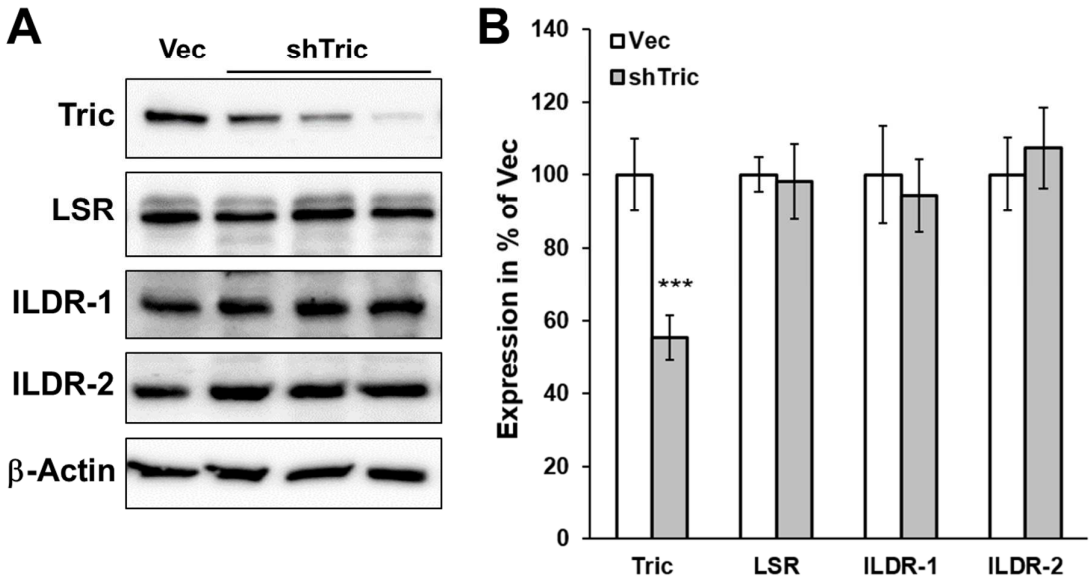

Fig. S3

A. Representative western blots showing Tric, LSR, ILDR-1 and ILDR-2 expression in selected shTRIC clones, which differed distinctly in their tricellulin expression. **B.** Densitometric analysis of protein expression levels in stable shTRIC transfectants in comparison to vector-transfected controls. Although all shRNA constructs lead to decreased tricellulin expression, no effect on angulin expression occurred (Tric: Vec: 100±10%, n=6; shTric: 55±6%, n=12, ***p<0.001; LSR: Vec: 100±7%, n=6; shTric: 98±11%, n=12; ILDR-1: Vec: 100±14%, n=6; shTric: 94±9%, n=12; ILDR-2: Vec: 100±10%, n=6; shTric: 107±12%, n=12;).

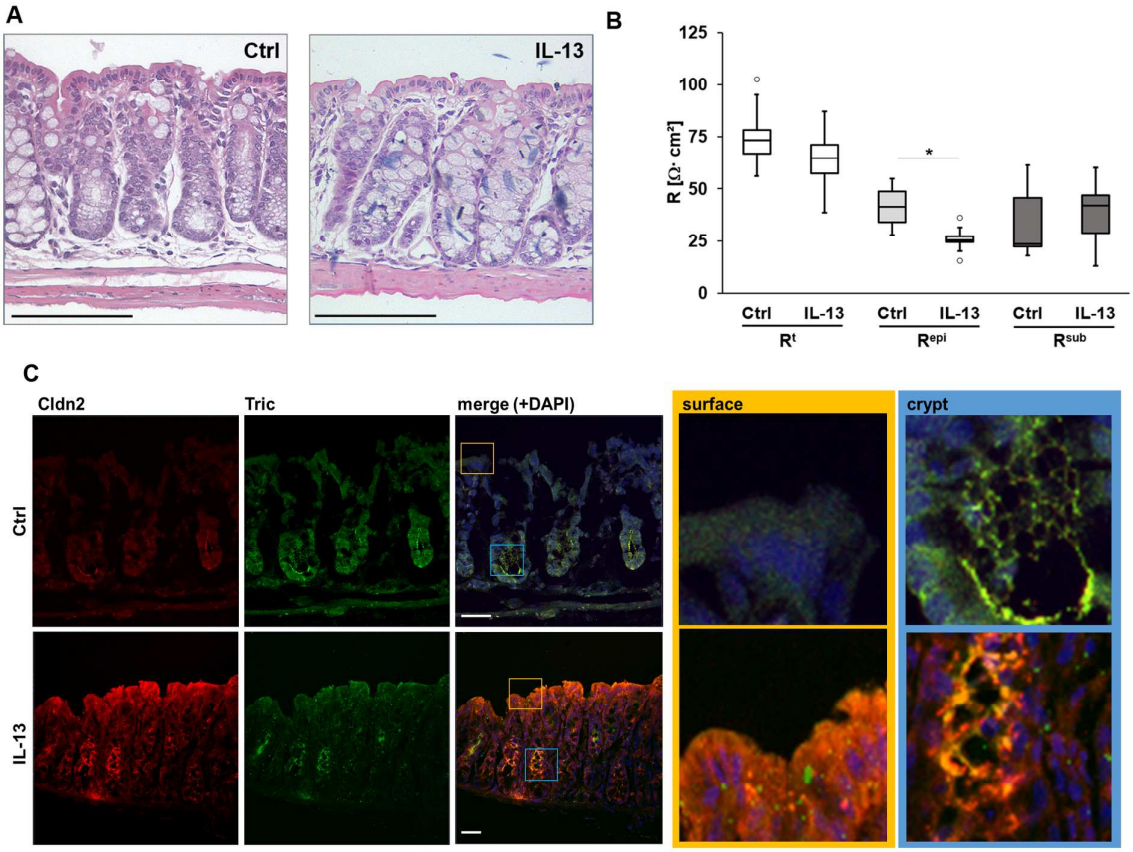

Fig S4

A. Representative HE staining of colonic tissue of untreated and IL-13-treated mice. No obvious changes were visible in crypt structure, mucosa and submucosa. Bar = 100 nm. **B.** Electrical resistances of colon tissue of untreated and IL-13-treated mice derived from impedance spectroscopic measurements. While the epithelial resistance (R_{epi}) is decreased (*$p<0.05$), the subepithelial resistance (R_{sub}) and transepithelial resistances (R_t) remained unchanged after treatment with IL-13 (n=5). **C.** Representative immunofluorescent staining of cryosectioned colonic tissue of untreated and IL-13-treated mice. An increase of claudin-2 (red) was observable after IL-13-treatment as claudin-2 also appeared in surface areas. The decrease of tricellulin signals was difficult to estimate only by analyzing the stainings – however, the images indicated that no shift in localization of tricellulin occurred, which also can be seen in the magnifications of surface epithelium (yellow box) and crypts (blue box). Bar = 50 µm.

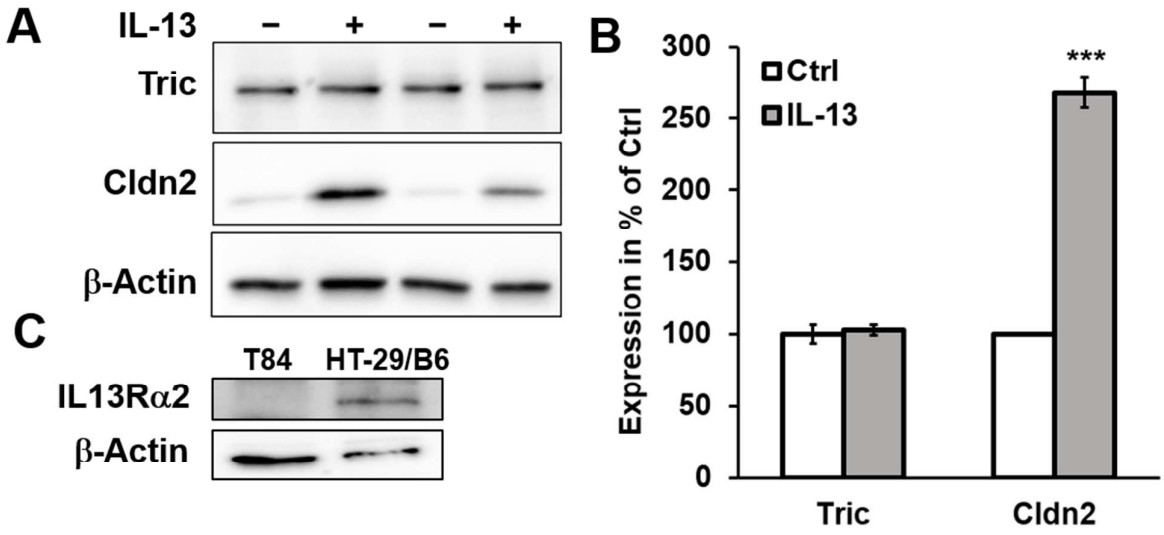

Fig. S5

A. Representative western blots of IL-13-treated T84 cells. **B.** Densitometric analysis of IL-13-treated T84 cells. Tricellulin expression is not effected by IL-13, while claudin-2 is upregulated (*$p<0.05$, $n=4$). **C.** Exemplary western blots showing IL-13Rα2 expression in HT-29/B6 cells, but not in T84.

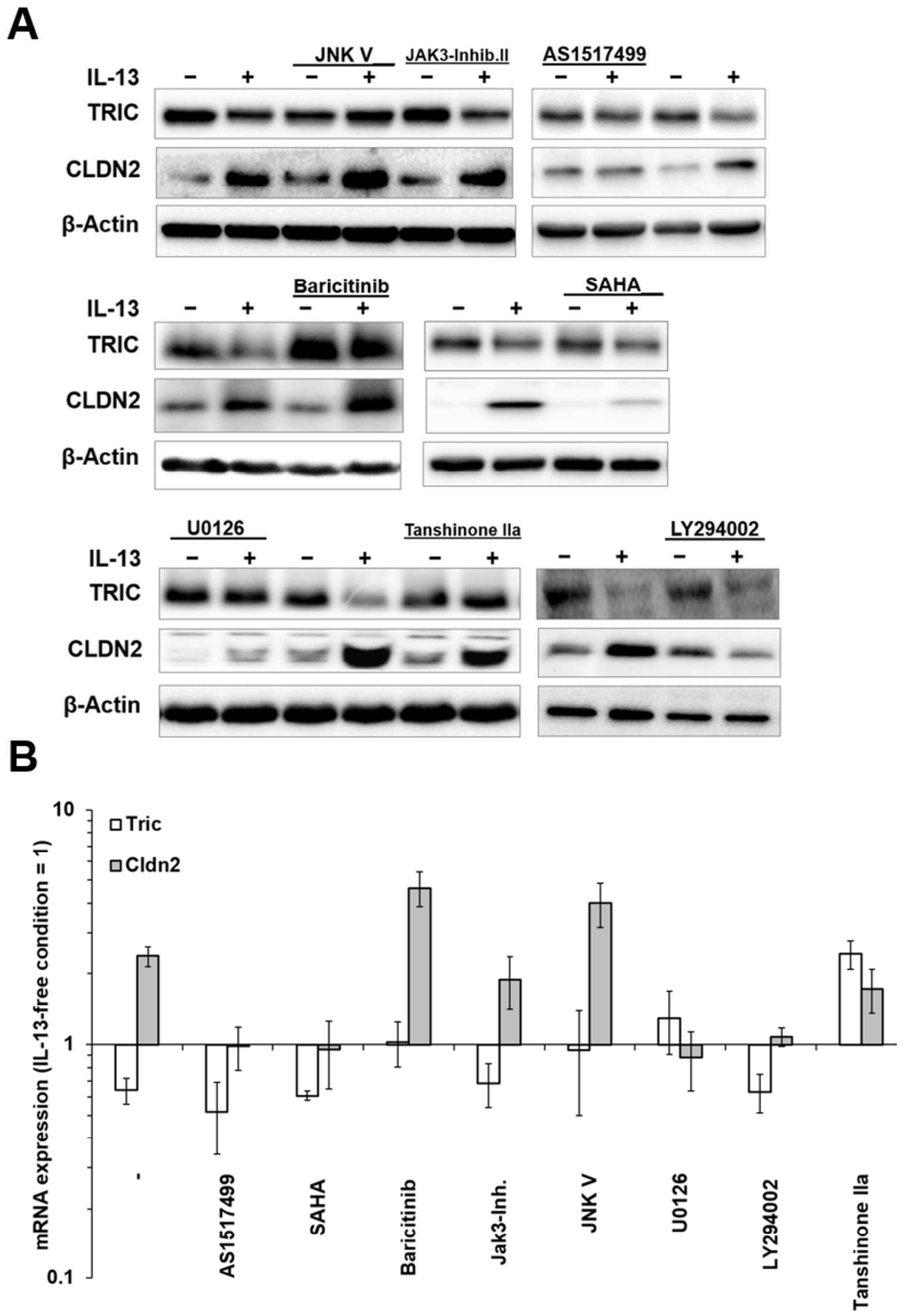

Fig. S6

A. Representative western blots of HT-29/B6 pretreated with different inhibitors before application of IL-13 showing tricellulin, Cldn2 and β-Actin as loading control. **B.** mRNA expression of tricellulin and claudin-2 in HT-29/B6 cells pretreated with different inhibitors before application of IL-13 (n=3-6).

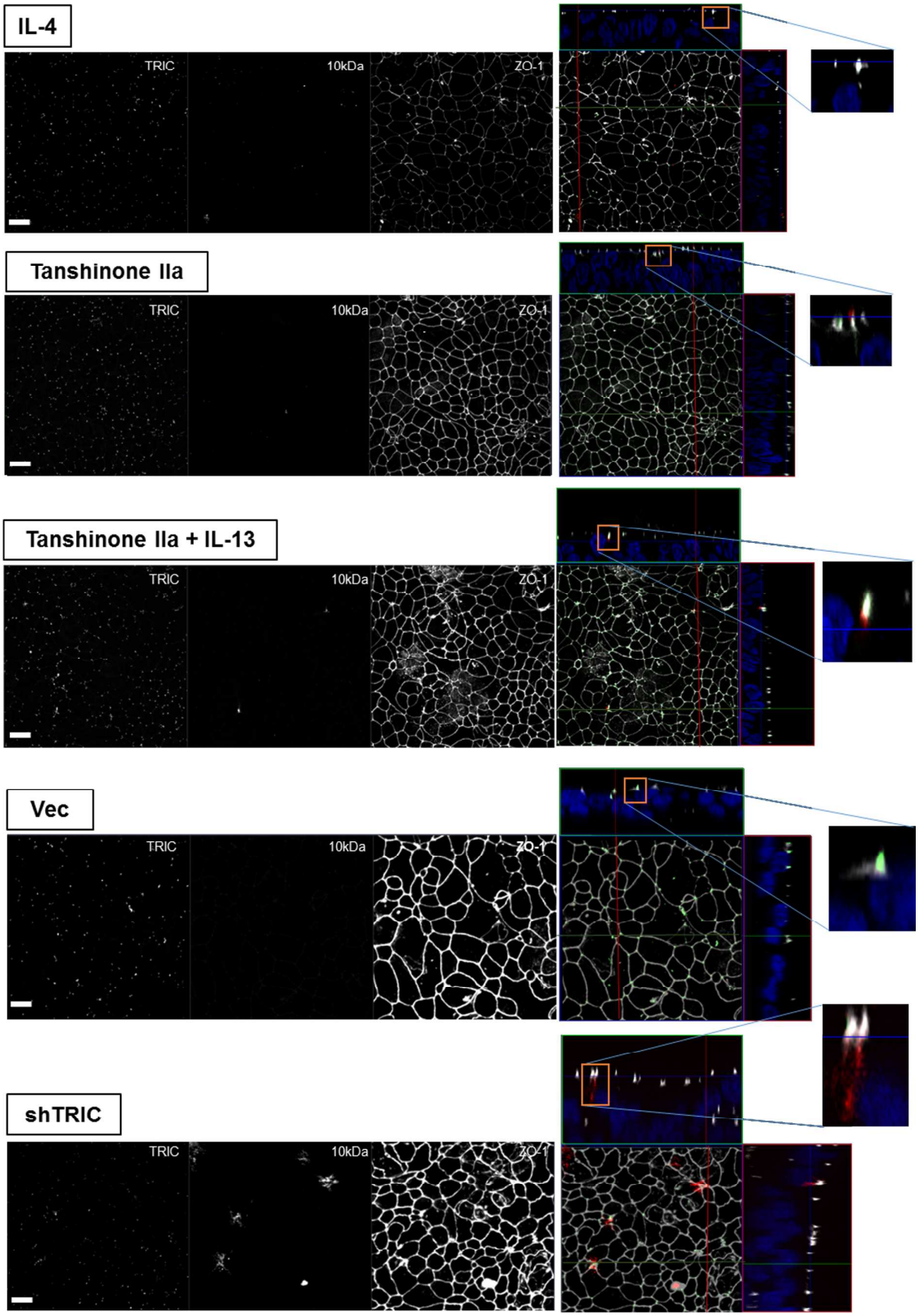

Fig. S7

Maximum intensity projections and Z-Stacks of exemplary immunofluorescence stainings of either treated with IL-4, Tanshinone IIa or Tanshinone IIa+IL-13 HT-29/B6 cells or HT-29/B6

cells transfected with empty vector or shTRIC. Cells were successively incubated incubated basolaterally with avidin and apically with biotin- and TRITC-labelled 10 kDa-dextran (middle, red in Z-stack). Tricellulin (left, green in Z-stack) and ZO-1 (right, gray in Z-stack) were counterstained for localization of the macromolecular passage. In the merge image, tricellulin signals were increased in contrast, while the ZO-1 signals were decreased for better evaluation of tricellulin localization. Bar = 20 μm.

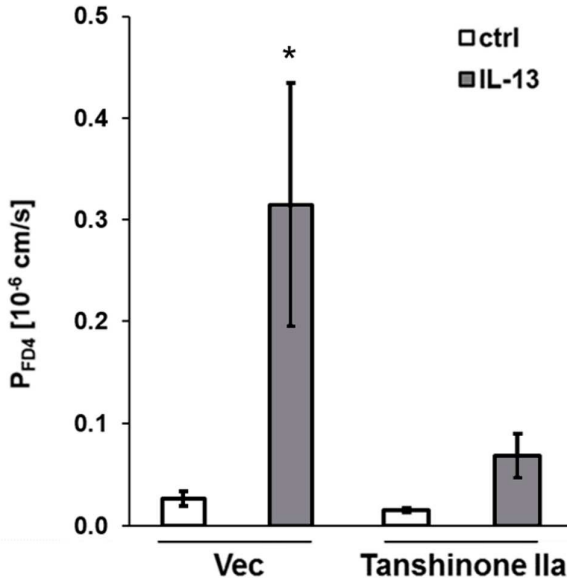

Fig. S8

Permeability for the macromolecular paracellular fluxmarker 4 kDa-FITC dextran in HT-29/B6 cells. Permeability is increased by IL-13, while pretreatment with tanshinone IIa does not result in an increase of FD4 permeability (Vec: 0.03±0.01 cm/s, n=7; IL-13: 0.31±0.12 cm/s, n=6; tanshinone IIa: 0.02±0.01 cm/s, n=3; tanshinone IIa + IL-13: 0.07±0.02 cm/s, n=3; *$p<0.05$).

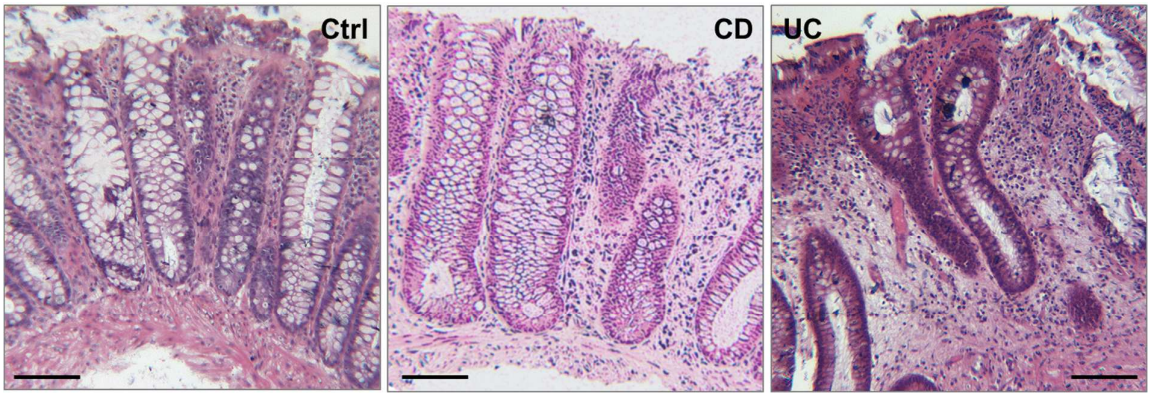

Fig. S9

Representative HE-staining of colonic tissue of Ctrl patients and patients with CD or UC. Bar = 100 nm.

Tab. S1

Effects of IL-13 on apoptotic rate, mRNA levels of tricellulin and claudin-2, protein and mRNA stability of tricellulin

	Ctrl		IL-13	
	mean	SEM	mean	SEM
apoptotic rate [%], n=3	2.00	0.07	1.75	0.10
protein stability of tricellulin; $T_{1/2}$ [h], n= 6	35.7	5.7	37.3	8.0
mRNA stability of tricellulin; $T_{1/2}$ [h], n= 4	10.8	1.2	9.9	2.2
mRNA level of tricellulin [% of Ctrl], n= 6	100	-	64	8
mRNA level of claudin-2 [% of Ctrl], n= 6	100	-	238	24

Supplementary Movie

First part: 3D-animation of control and IL-13-treated HT-29/B6 cells. Cells were immunofluorescence stained against ZO-1 (gray) and Tric (green) after incubation with biotin- and TRITC-labeled 10 kDa-dextran (red) which was captured after passage of the TJ by avidin with which the cells basolaterally were covered before the experiment. In controls, no passage of 10 kDa dextran was detectable below the TJ after one hour of incubation. When treated with IL-13, signals of 10 kDa dextran were detectable below tricellular TJs.

Second part: 3D-animation of vector controls and shTRIC-transfected HT-29/B6. Cells were immunofluorescence stained against ZO-1 (gray) and Tric (green) after incubation with biotin- and TRITC-labeled 10 kDa-dextran (red) which was captured after passage of the TJ by avidin with which the cells basolaterally were covered before the experiment. In vector controls, no passage of 10 kDa dextran was detectable below the TJ after one hour of incubation, while clear passage of the 10 kDa dextran was detectable below tTJs in shTRIC cells.